

AD-A069 304

SRI INTERNATIONAL MENLO PARK CA

F/G 17/5

A SYSTEM DESCRIPTION OF AN IMPROVED 10.6-MICROMETERS LIDAR SYST--ETC(U)

APR 79 J E LAAN

DAA629-77-C-0001

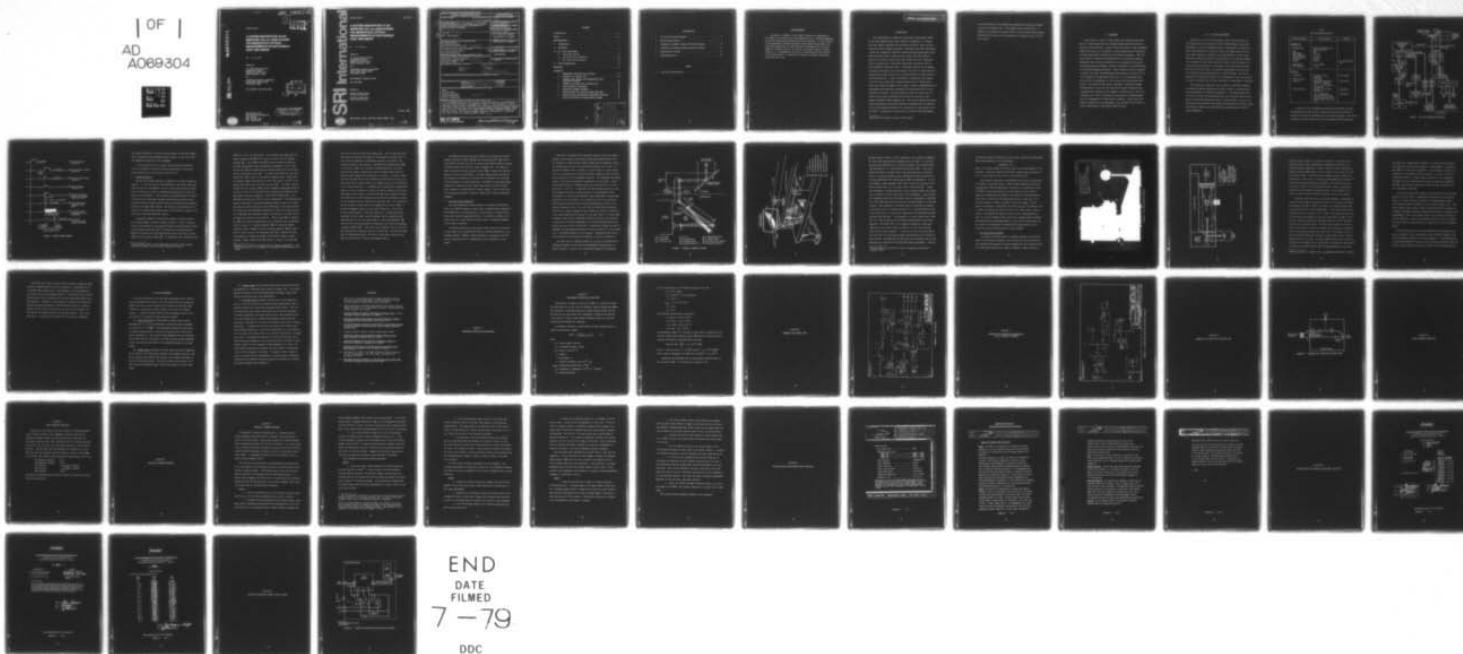
UNCLASSIFIED

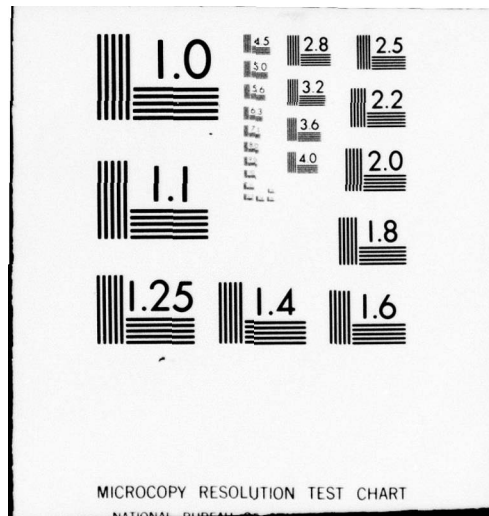
TR-2

ARO-13833,3-6S

NL

OF
AD
A069304





ARO 73833.3-GS

(15)

LEVEL

Technical Report 2

**A SYSTEM DESCRIPTION OF AN
IMPROVED 10.6 μ m LIDAR SYSTEM
FOR MONOSTATIC OPTICAL
MEASUREMENTS OF BATTLEFIELD
DUST AND SMOKE**

By: J. E. van der LAAN

Prepared for:

U.S. ARMY RESEARCH OFFICE
GEOSCIENCES DIVISION
RESEARCH TRIANGLE PARK
NORTH CAROLINA 27709

and

ATMOSPHERIC SCIENCES LABORATORY
WHITE SANDS MISSILE RANGE
NEW MEXICO 88002

ARO CONTRACT DAAG29-77-C-0001

DDC
JUN 4 1979
A

DDC FILE COPY



333 Ravenswood Avenue
Menlo Park, California 94025 U.S.A.
(415) 326-6200
Cable: SRI INTL MNP
TWX: 910-373-1246

DISTRIBUTION STATEMENT A

Approved for public release;
Distribution Unlimited

79 05 29 008



Technical Report 2

April 1979

A SYSTEM DESCRIPTION OF AN IMPROVED 10.6 μm LIDAR SYSTEM FOR MONOSTATIC OPTICAL MEASUREMENTS OF BATTLEFIELD DUST AND SMOKE

By: J. E. van der LAAN

Prepared for:

U.S. ARMY RESEARCH OFFICE
GEOSCIENCES DIVISION
RESEARCH TRIANGLE PARK
NORTH CAROLINA 27709

and

ATMOSPHERIC SCIENCES LABORATORY
WHITE SANDS MISSILE RANGE
NEW MEXICO 88002

ARO CONTRACT DAAG29-77-C-0001

SRI Project 5862

Approved by:

WARREN B. JOHNSON, *Director*
Atmospheric Sciences Laboratory

CHARLES A. SHOENS, *Director*
Systems Techniques Laboratory

Copy No.6....

333 Ravenswood Avenue • Menlo Park, California 94025 • U.S.A.

79 05 29 008

REPORT DOCUMENTATION PAGE		READ INSTRUCTIONS BEFORE COMPLETING FORM	
1. REPORT NUMBER		2. GOVT ACCESSION NO.	
		(Micrometers)	
3. RECIPIENT'S CATALOG NUMBER		(9)	
4. TITLE (and Subtitle)		5. TYPE OF REPORT & PERIOD COVERED	
A SYSTEM DESCRIPTION OF AN IMPROVED 10.6- μ m LIDAR SYSTEM FOR MONOSTATIC OPTICAL MEASUREMENTS OF BATTLEFIELD DUST AND SMOKE.		Technical Report 2 Covering the Period February 1978 to March 1979	
7. AUTHOR(s)		6. PERFORMING ORG. REPORT NUMBER	
Jan E. van der Laan		SRI Project 5862 ✓	
9. PERFORMING ORGANIZATION NAME AND ADDRESS		8. CONTRACT OR GRANT NUMBER(s)	
SRI International 333 Ravenswood Avenue Menlo Park, California 94025		Contr. DAAG29-77-C-0001 ✓ (15)	
11. CONTROLLING OFFICE NAME AND ADDRESS		10. PROGRAM ELEMENT, PROJECT, TASK AREA & WORK UNIT NUMBERS	
U.S. Army Research Office Geosciences Division Research Triangle Park, North Carolina 27709			
14. MONITORING AGENCY NAME & ADDRESS (if diff. from Controlling Office)		12. REPORT DATE	
Atmospheric Sciences Laboratory White Sands Missile Range New Mexico, 88002		April 1979	
		13. NO. OF PAGES	
		57 pages	
16. DISTRIBUTION STATEMENT (of this report)		15. SECURITY CLASS. (of this report)	
Approved for public release; distribution unlimited.		UNCLASSIFIED	
		15a. DECLASSIFICATION/DOWNGRADING SCHEDULE	
17. DISTRIBUTION STATEMENT (of the abstract entered in Block 20, if different from report)			
18. SUPPLEMENTARY NOTES			
THE VIEW, OPINIONS, AND/OR FINDINGS CONTAINED IN THIS REPORT ARE THOSE OF THE AUTHOR(S) AND SHOULD NOT BE CONSTRUED AS AN OFFICIAL DEPARTMENT OF THE ARMY POSITION, POLICY, OR DECISION, UNLESS SO DESIGNATED BY OTHER DOCUMENTATION.			
19. KEY WORDS (Continue on reverse side if necessary and identify by block number)			
LIDAR Military smoke Optical properties Optical backscatter Optical transmission		micrometers	
20. ABSTRACT (Continue on reverse side if necessary and identify by block number)			
A 10.6- μ m wavelength CO ₂ lidar system, designed specifically for measurements of battlefield dust and smoke, was installed in the U.S. Army Atmospheric Sciences Laboratory's laser Doppler velocimeter van. The system design addresses recommendations made following a smoke test field program using a prototype system at Dugway Proving Ground in September 1977. Improvements in range resolution, range jitter, side lobe clutter, and amplitude dynamic range were incorporated in the system. This report serves as a system technical manual.			

CONTENTS

ILLUSTRATIONS	iv
TABLES.	iv
ACKNOWLEDGMENTS	v
I INTRODUCTION	1
II BACKGROUND	3
III ASL LIDAR DEVELOPMENT.	4
A. System Description.	8
B. ASL Lidar Laser Transmitter	11
C. ASL Lidar Receiver System	16
IV SYSTEM IMPROVEMENTS.	22
REFERENCES.	24
APPENDICES	
A PERFORMANCE PREDICTION CALCULATIONS	25
B SCHEMATIC FOR CONTROL UNIT.	28
C SCHEMATIC FOR TRIGGER AND SYNCHRONIZED PULSE ISOLATION INTERFACE	30
D SCHEMATIC FOR FIBER OPTIC DETECTOR UNIT	32
E LASER OPERATING CONDITIONS.	34
F RECEIVER ALIGNMENT PROCEDURE.	36
G SPECIFICATIONS FOR RECEIVER LINEAR AMPLIFIER.	42
H SPECIFICATIONS FOR RECEIVER LOGARITHMIC AMPLIFIER	47
I RECEIVER ELECTRONICS PACKAGE WIRING DIAGRAM	51

Accession For	<input checked="checked" type="checkbox"/> <input type="checkbox"/> <input type="checkbox"/>	DTIC GRA&I DDC TAB Unannounced Justification	By	Distribution/	Availability Codes	Availand/or special
						Dist. A

ILLUSTRATIONS

1	ASL Lidar Functional Diagram	6
2	System Timing Diagram.	7
3	Transmitter Alignment Package Functional Diagram	13
4	Transmitter Alignment Package Conceptual Drawing	14
5	LIDAR Receiver Package	17
6	ASL/LIDAR Receiver	18

TABLES

1.	ASL Lidar Specifications	5
----	------------------------------------	---

ACKNOWLEDGMENTS

The author is indebted to Dr. Edward R. Murray for assistance in the design of the improved CO₂ lidar system and to Dr. Richard Baumgartner for helpful discussions concerning system calculations. Dr. Ray Loveland of the Atmospheric Sciences Laboratory, White Sands Missile Range, provided many suggestions on system interface requirements with the laser Doppler velocimeter system. In addition, the author wishes to acknowledge Dr. J. S. Randhawa for his work in coordinating the field evaluation program and Mr. K. Ballard and R. March for technical assistance during the field test.

I INTRODUCTION

SRI International is conducting a three-year investigation funded by the Army Research Office (ARO), Division of Geophysics, to develop real-time digital techniques for evaluation of aerosol, cloud, and precipitation optical physical densities. Consistent with these objectives, a field test program was conducted at Dugway Proving Grounds where lidar observations were made of smoke and dust clouds using SRI's Mark IX lidar ($0.7\text{ }\mu\text{m}$) and a prototype CO_2 lidar system ($10.6\text{ }\mu\text{m}$)¹. Additional funds to support part of this field program were provided by the U.S. Army Atmospheric Laboratory (ASL). The primary objective of the Dugway test was an evaluation of the performance of the $10.6\text{ }\mu\text{m}$ lidar system for observations of smoke rather than a detailed analysis of smoke distributions and densities. It was not possible to characterize and evaluate fully the $10.6\text{ }\mu\text{m}$ lidar from a systems approach due to limited operational time during the Dugway tests; however, several recommendations for improvement were identified, providing the design objectives for an improved $10.6\text{-}\mu\text{m}$ system. The ASL provided the funds to develop this improved $10.6\text{-}\mu\text{m}$ lidar system which was installed in the ASL's Laser Doppler Velocimeter (LDV) equipment van. This report provides a detailed system description and outlines operational procedures for the improved $10.6\text{-}\mu\text{m}$ lidar system, henceforth to be referred to in this report as the ASL lidar. In addition to, and as part of, this ASL lidar development,

¹References are listed at the end of this report.

a second evaluation field program was scheduled with objectives similar to those in the Dugway test. This program, Dusty Infrared Test - 1 (DIRT-1), was conducted in October 1978 at the White Sands Missile Range, New Mexico; the results will be presented in a separate report on this ARO contract.

II BACKGROUND

Lasers provide a source of light energy with characteristics necessary for strong interaction with atmospherically-suspended particulate matter at remote distances. Using a pulsed laser source, radar techniques (lidar-laser radar) can be applied to provide range-resolved information of these interactions by observing the backscatter signature. With certain auxiliary information and appropriate data processing techniques, backscatter and extinction coefficients can be measured for naturally-occurring aerosols, providing a reference background for characterization of artificially-generated aerosols. Recent military interest in methods to measure real-time, three-dimensional distributions of density and optical parameters of dense smoke clouds led to a two-wavelength lidar (0.7 and 10.6 μm) experiment to collect basic data on generated smoke clouds. The results of this initial experiment, conducted at Dugway Proving Grounds in late 1977 with ARO and ASL support, generally were consistent with theoretical data relating to aerosol particle size distributions, and clearly illustrated the usefulness of long-wavelength lidar for measurements of large particle aerosols. These results provided the stimulus for the development of an improved 10.6- μm lidar for optical measurements of battlefield smoke and dust.

III ASL LIDAR DEVELOPMENT

Evaluations of the 10.6 μm -wavelength lidar operation during the 1977 Dugway field test identified several system parameters requiring improvement in the next generation system. Optimization of range resolution and elimination of side-lobe clutter and timing jitter were the major design objectives addressed in the development of the ASL lidar. The system originally proposed for installation in the ASL-LDV equipment van² included the lidar laser transmitter system, receiver system, and a data digitizing system to be interfaced to the data processing equipment van of the LDV system. The receiver system would use the 12-inch $f/2$ telescope and beam steering optics of the LDV system. The ASL requested SRI to design the system so that minimum effort would be required to convert operation from the lidar mode back to the LDV mode of operation.

SRI designed and installed a lidar system in the ASL-LDV equipment van having the general specifications given in Table 1; system performance calculations are discussed in Appendix A. The system design does not alter the normal LDV operational mode in any way except that the LDV cannot be operated simultaneously with the lidar system; in fact, if the LDV system were operational and aligned, the lidar mode of operation could be installed, operated, and removed without disturbing any of the LDV system alignments.

Table 1
ASL LIDAR SPECIFICATIONS

System Component	Specification	Comments
<u>Transmitter</u>		
Manufacturer	Lumonics Research Ltd., Model TEA-101-2	No nitrogen gas mix
Type	CO ₂	
Wavelength	10.6 μm	
Beam diameter	3.1 cm	
Beam divergence	1.2 mrad	
Operation	pulsed	
Energy	250 mJ	
Pulsewidth	75 ns (FWHM)	
PRF (maximum)	1 pps	
<u>Receiver</u>		
Telescope	12-inch (30 cm), Newtonian	LDV primary
Field of view	1.23 mrad	
Detector	Honeywell Associates; HgCdTe photodiode; $D^* = 1.3 \times 10^{10} \text{ cm}^2 \text{ Hz}^{-1}$; 100 MHz BW	LN ₂ -cooled
Post amplifier	linear: 26 dB gain, 100 MHz BW log: tangential sensitivity -111 dBr; ±0.5 dB linearity over 80-dB range; 15-ns rise time	Appendix G Appendix H

In addition to the abovementioned objectives and design criteria, SRI designed the system so that a minimum effort would be required to prepare the system for transportation to new field locations. All system components are shock-mounted, and special shipping brackets were made

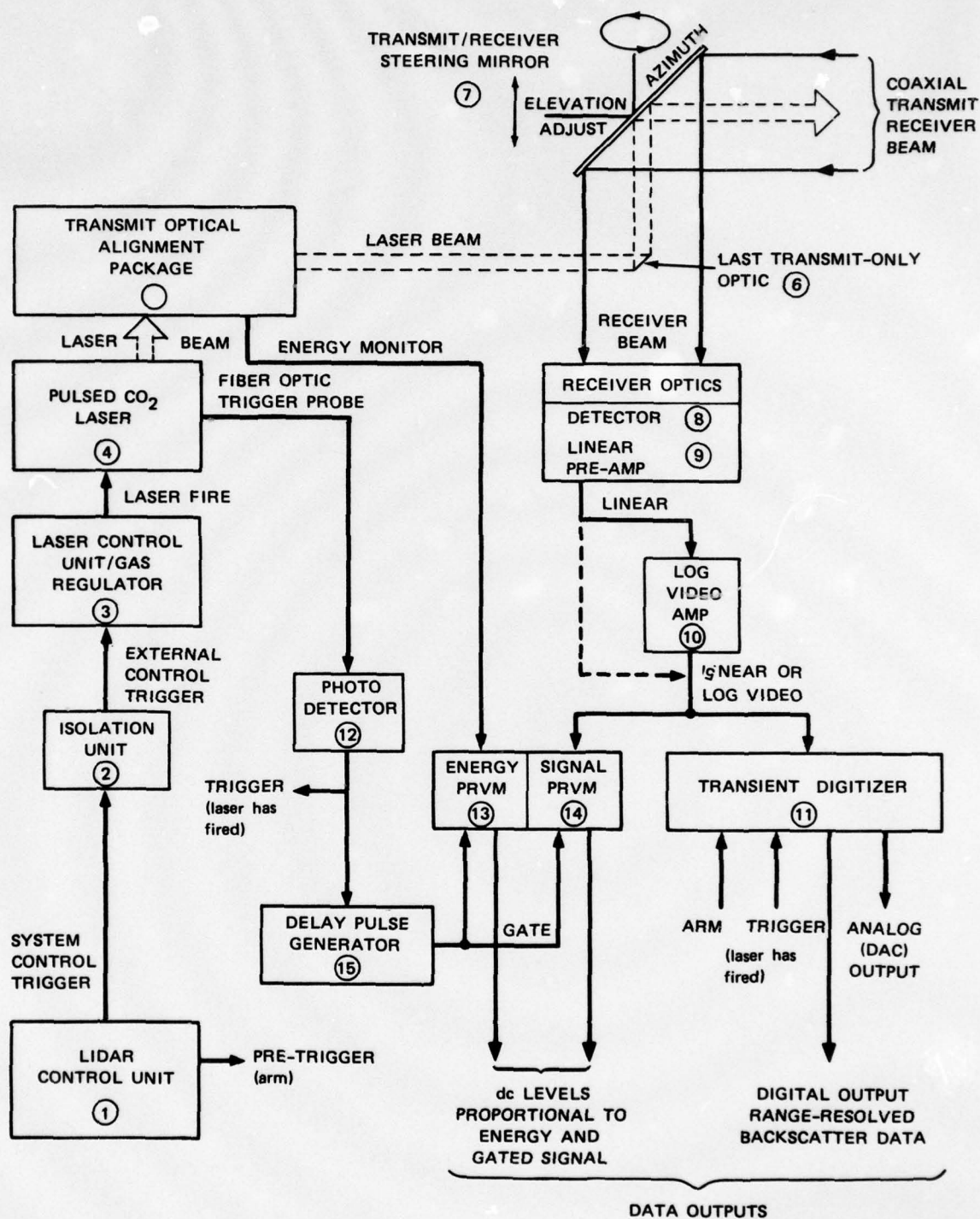


FIGURE 1 ASL LIDAR FUNCTIONAL DIAGRAM

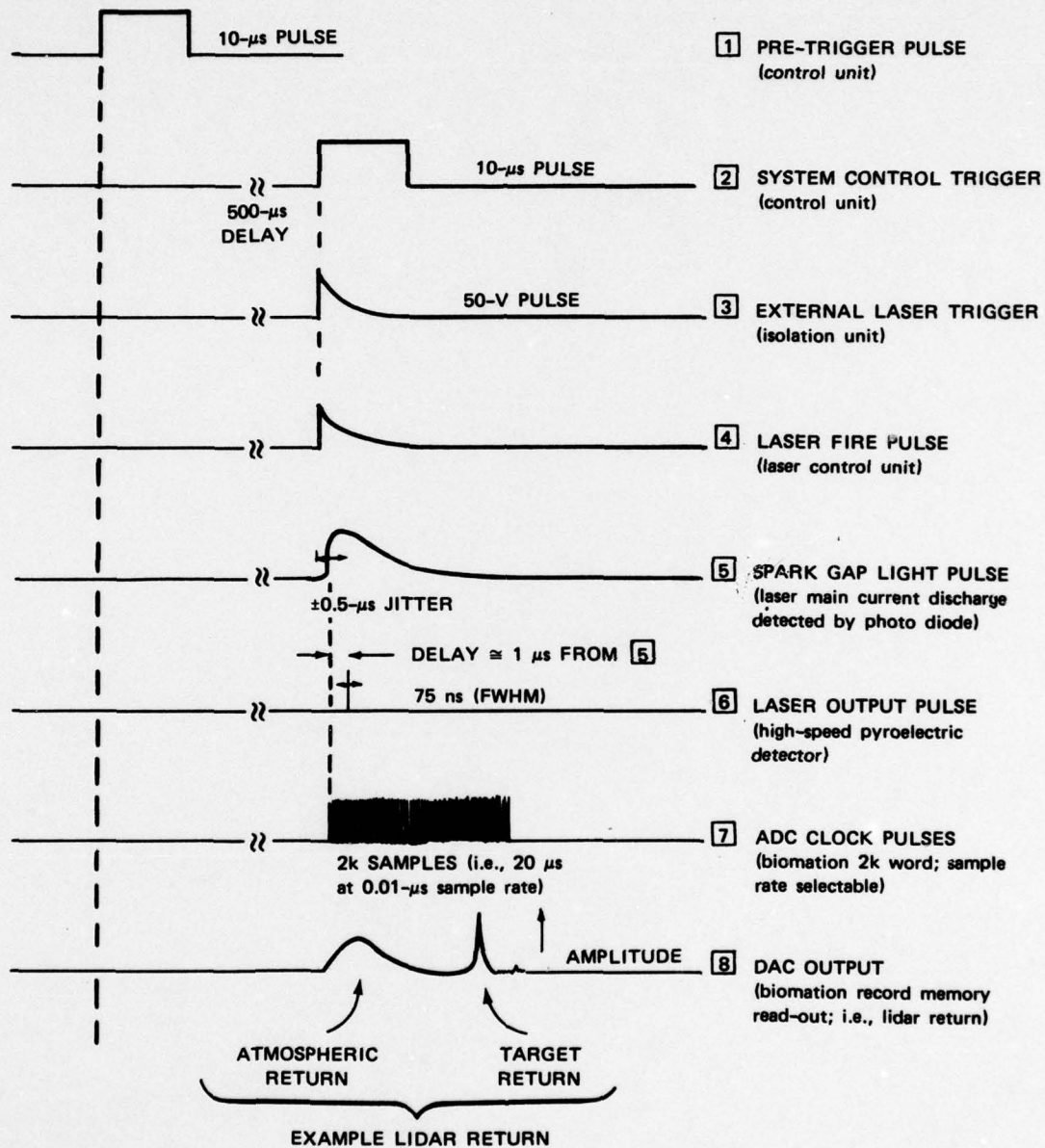


FIGURE 2 SYSTEM TIMING DIAGRAM

for quick installation. The van also was modified for air-ride suspension to anticipate system shipment without removal of any of the optical components requiring critical alignment.

In the discussion below, a general system description (Section III A) is presented, followed by detailed descriptions of the transmitter (Section III B) and receiver (Section III C).

A. System Description

The ASL lidar system basically is composed of two major system components: (1) a pulsed CO₂ laser that generates a very short, high peak power IR pulse for transmission, and (2) a narrow field-of-view optical receiver system that collects the backscattered energy and directs the signal to an IR detector. After detection and amplification, the signal is digitized by a high-speed transient recorder which provides range-resolved backscatter amplitude data output in both digital and digitally-reconstructed analog (DAC) formats. The digital output primarily is intended for recording and processing while the DAC output is useful in observing the real-time backscatter returns.

A functional diagram of the ASL lidar system is shown in Figure 1 and a timing diagram of events is shown in Figure 2. Refer to Figures 1 and 2 for elucidation of the system functions description which follows. A lidar system control unit (1) * (constructed by SRI and detailed in Appendix B) generates two line-synchronized control functions, pre-trig [1] and system control trigger [2], at selectable pulse repetition rates

* Circled numbers refer to items identified in Figure 1 while numbers enclosed in squares refer to timing functions in Figure 2.

(PRFs) of 1, 1/2, 1/4, and 1/8 Hz. The pretrigger pulse [1] leads the control trigger pulse [2] by 500 μ s and is used to arm the transient recorder (11). The trigger pulse [2] is routed through an isolation unit (2) (constructed by SRI and detailed in Appendix C) to the laser control unit (3) and provides ground isolation between the laser system and the system control unit (1). In lidar system operation, the laser control unit (3) is used in the external triggering mode. Reception of an external trigger synchronizes the laser fire control circuits of the normal laser control unit and fires the laser [4]. The laser output is directed via the transmit (XMIT) optical alignment package (5) (detailed in Section III B) to the last XMIT optic steering mirror (6) where the XMIT beam is directed, coaxially to the receiver (RCVR) beam, to the XMIT/RCVR steering mirror (7) for output transmission.* The backscattered signals, generated by scattering mechanisms along the path of the laser beam that are within the field-of-view (RCVR beam) of the lidar receiver, are directed via the XMIT/RCVR steering mirror (7) to the receiver optical system (8). The backscatter energy is collected by a 12-inch (30 cm) telescope and focused on an IR detector. Either linear (9) or logarithmic (10) post-detection amplification can be selected, and the amplified video is routed to a transient digitizer (11) for analog-to-digital conversion (ADC). Remember that the transient digitizer (11) was armed prior to laser firing by the pretrigger pulse [1], meaning that digitizer memory was cleared and control circuits were readied to begin sampling. When a trigger pulse [6] (laser has fired) is received, ADC

* Alignment of the XMIT and RCVR beam will be covered in Appendix B. For the discussion here, it is assumed that the XMIT and RCVR beams are converged.

will occur on the next 2048 clock samples [7] . This 2K data word automatically is placed into the memory of the transient recorder where it can be read out digitally for permanent storage or processing. The transient digitizer also provides a repetitive DAC sampling output [8] of the data in memory for convenient A-scope monitoring of the data. The data will remain in memory and cannot be updated again until the next arm pulse-trigger/pulse combination is received. In order to time-lock the start-ADC time for the transient recorder with the actual laser pulse start time (no range jitter), the trigger pulse must be referenced to the actual laser pulse. A convenient way to derive this trigger pulse would be to use a pyroelectric detector to detect a sample of the actual laser pulse output; however, we have found that radio frequency interference (RFI) from the laser firing easily can enter the pyroelectric detector and interfere with the detection of real-time zero. This problem was the major cause of range jitter on the Dugway 10.6- μ m lidar system. A preferred triggering system for zero-time reference is a fiber optic pick-up placed adjacent to the laser spark gap. A strong light pulse, coincident with the laser current discharge, can be transmitted over long distances via the fiber optic cable to a fast PIN photodiode (12) (constructed by SRI and described in Appendix D) for detection providing a trigger reference [6] . This fiber optic technique is free of RFI and also eliminates one potential source of ground loops. The detected light pulse is synchronized within 10 to 20 ns of the actual laser pulse and leads the laser pulse in time by approximately 500 ns.

In addition to the basic system elements just described, two peak-reading voltmeters³ (PRVM) ⑬ ⑭ and a delay generator⁴ ⑮ are incorporated in the ASL lidar both to provide a convenient method of observing laser energy output and as a system alignment aid. The PRVMs are gated in time by the delay generator output ⑮ to sample only specific regions of data for peak signals. The peak reading detected during the gate period is converted to a DC level that is available for recording and is displayed on a front panel meter. One PRVM is used during normal operation to observe the laser energy output while the other monitors select ranges of received video for desired targets. This is quite useful in steering the lidar to specific targets and in system convergence alignment.

B. ASL Lidar Laser Transmitter

The laser transmitter system consists of a Lumonics CO₂ TEA-101-2 laser, an alignment package to enable rapid, straightforward alignment of the transmitter, an on-line monitor of laser energy on a pulse-to-pulse basis, and a system triggering interface. The system is mounted on the bottom level of a sturdy two-level optical table to maintain alignment of the various components.

A detailed description of the Lumonics laser will not be presented in this report as its operation and theory is covered adequately in its equipment manual.⁵ However, details pertinent to operation of the ASL lidar in particular will be discussed here and in Appendix E of this report.

The laser is operated with an unstable resonator cavity in order to provide a low-divergence beam without using beam-expanding optics that are difficult to align and that require larger and more expensive optics. The unstable optics yield a far-field beam divergence of 1.2 mrad. Although the Lumonics laser is capable of several joules of output energy, this is not achievable when using the unstable resonator optics and operation optimized for short pulsewidth operation. The pulsewidth and energy output of the laser is adjustable depending on the gas mixture. With a gas mixture adjusted for maximum energy, the pulse consists of a 75-ns spike with a 1- μ s tail. By operating the laser without N_2 the 1- μ s tail is eliminated, but with an energy reduction to approximately 250 mJ. Fortunately, our test with the TEA-101-2 laser showed that the peak power contained in the 75-ns spike is not affected by the zero N_2 operation. This condition exists because of the time-dependent gain curve of the unstable resonator cavity. The cavity gain is insufficient during the first 75 ns to support lasing with N_2 ; therefore, N_2 does not contribute to the laser energy during this part of the laser pulse.⁶ For high range resolution lidar this is a desirable operating condition, but stability of operation is critically dependent on an optimized He/CO₂ mixture and proper flow rate for the selected PRF. A significant attempt was made to determine the appropriate conditions for stable operation at a 1-Hz firing rate; < $\pm 5\%$ energy stability can be achieved. Appropriate laser operating conditions for achieving this stability are given in Appendix E.

The laser output is guided by means of a series of infrared optics (alignment package) to the lidar system XMIT/RCVR steering mirror as shown in Figure 3. Figure 4 is a conceptual drawing of the alignment

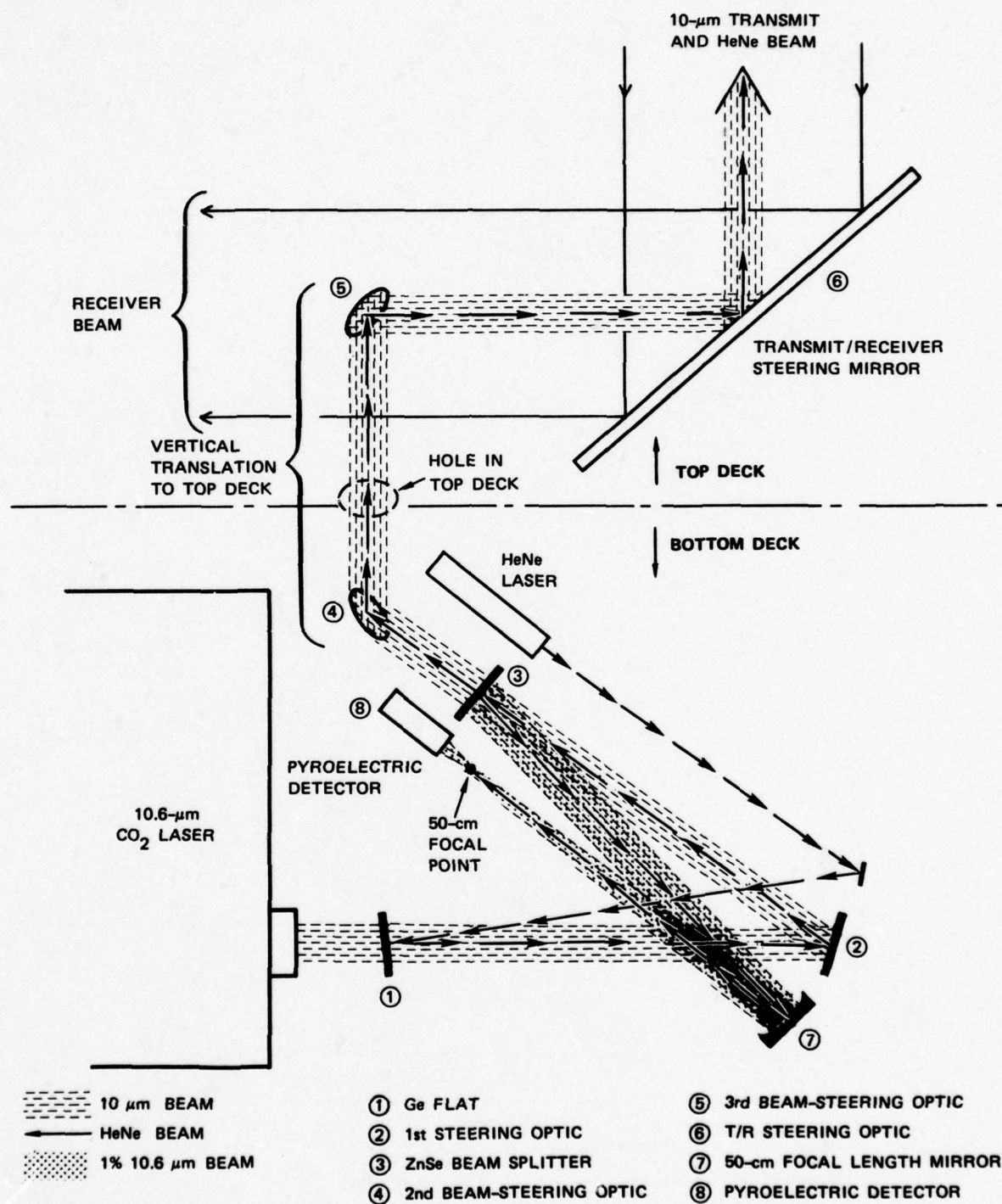


FIGURE 3 TRANSMIT ALIGNMENT PACKAGE

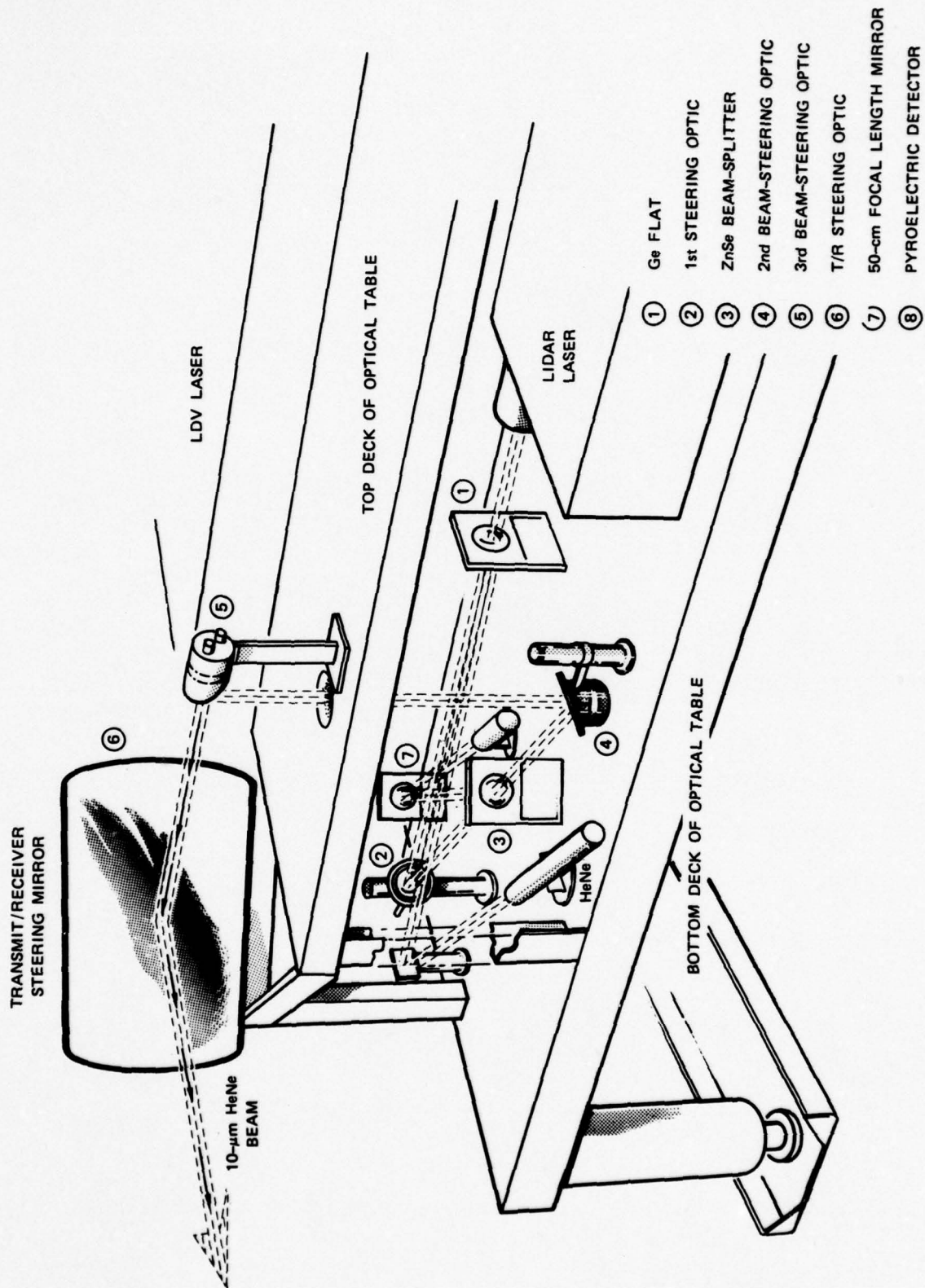


FIGURE 4 TRANSMIT ALIGNMENT PACKAGE (conceptual drawing)

package that may provide a better perspective of the optical arrangement. The laser beam passes through a germanium (Ge) flat (1) * to the first steering mirror (2) where it is directed through a zinc selenide (ZnSe) (3) beam-splitter to a second beam-steering mirror (4). This mirror directs the beam up through a hole in the second level of the optical table to a third beam-steering optic (5) where the beam is directed to the lidar XMIT/RCVR (T/R) steering mirror (6) for transmission. To aid in alignment, a HeNe alignment laser⁷ beam is placed on axis with the IR beam by reflecting it off the output side of the Ge flat (1). Using this arrangement, the HeNe beam may be left on during normal laser operation to provide a visible indication of the IR beam path. Exact parallel axis alignment between the IR and HeNe beam is accomplished by adjusting the Ge flat (1) positioning such that the far-field beams are in the same location. This alignment is performed easily by observing the position of an IR burn spot on a suitable material (i.e., uncoated Polaroid film) at the focal point of a 50-cm focal length mirror and adjusting the HeNe beam onto this burn spot. This alignment, of course, should not be done with full laser energy as the full-focused energy density can be quite dangerous. The method used in our alignment package is to beam split (3) off 1% of the laser energy and direct it at the 50-cm focusing mirror (7) as shown in Figure 3. A burn spot at the focal point (7) of the 50-cm mirror can be detected easily and represents the far-field IR beam location. The HeNe beam far-field spot can be adjusted onto the IR beam burn spot using the Ge flat (1) Gimbal mount adjustments. The burn

* Circled numbers in Section III B refer to components identified in Figures 3 and 4.

spot derived using this method also can be used to define the approximate laser beam divergence by the relationship:

$$\text{Divergence} = d/F$$

where F = the focal length of the lens, and d = spot-size diameter at $1/e$ intensity. Using this method the ASL lidar transmit beam is measured to be < 1.5 mrad, which is very close to the specified value.

Laser energy is measured on an individual pulse basis by monitoring a 1% sample of each laser pulse. Using the same beam-splitter (3) and focusing mirror (7) described above, a Molelectron J-3 pyroelectric detector⁸ (8) is placed approximately one inch beyond the focal point to sample the transmitted pulse energy. The detector is placed beyond the focal point to distribute the energy density over a large area of the detector chip and to reduce the chance of detector damage. Several layers of low-density polyethylene are used in front of the detector chip in order to attenuate the level of input to the linear range of the detector. The pyroelectric detector output then is calibrated with respect to a disc colorimeter laser power meter (Sciencetech Model 36-0401).⁹ The pulse-to-pulse energy measurement is very useful in normalizing target returns for computations of transmittance through smoke or dust clouds and in early identification of laser problems.

C. ASL Lidar Receiver System

In response to the ASL request to minimize downtime in converting back to the LDV mode of operation and to utilize the LDV system receiving telescope, SRI designed a detector package that can be removed quickly, allowing LDV operation in a matter of minutes. When the detector

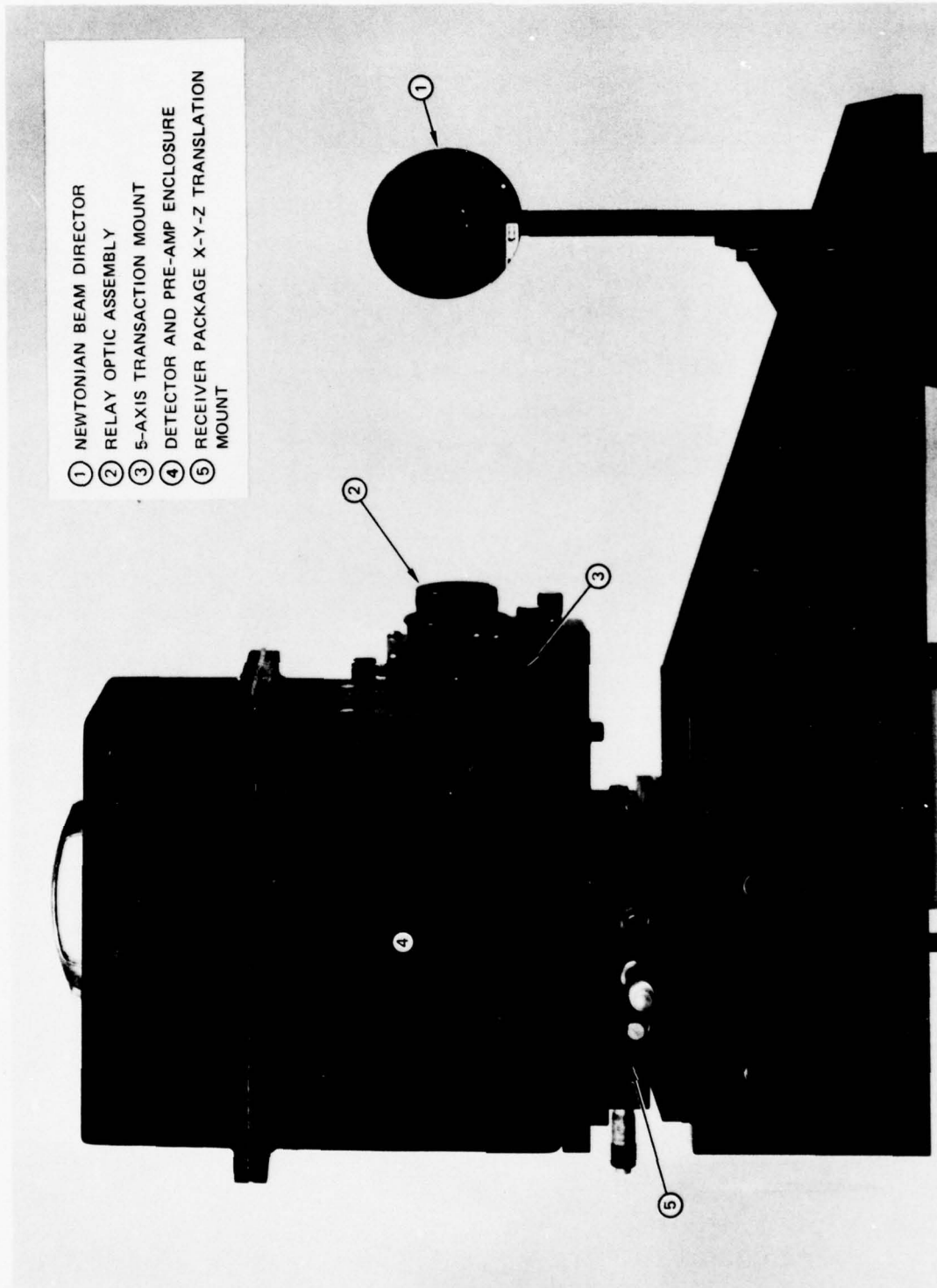


FIGURE 5 ASL LIDAR RECEIVER PACKAGE

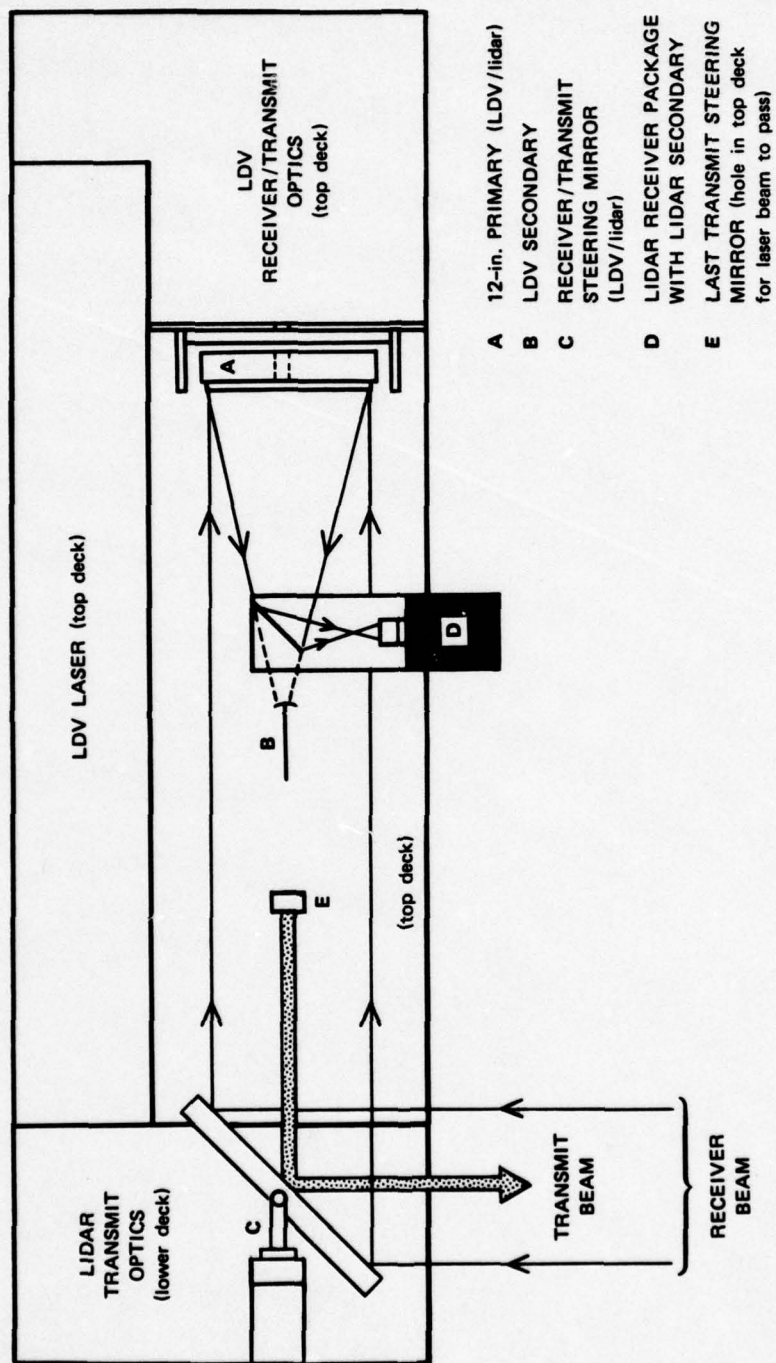


FIGURE 6 ASL LIDAR RECEIVER

package, shown in Figure 5, is placed in position, it converts the receiving telescope from a Cassegrainian configuration (LDV mode) to a Newtonian system (LIDAR mode). Figure 6 shows the major receiving components for both systems which all are located on the top deck of a two-level optical table. The lidar detector package contains a Newtonian beam-director, relay optics, a liquid N_2 -cooled HgCdTe diode detector,¹⁰ and post-detection amplification electronics. The detector and electronics are located in an RFI-shielded enclosure that is conductively-isolated from the assembly by phenolic mounts. This isolation is required to ensure receiver isolation integrity from the laser ground.

In the lidar operation mode, the receiver package is positioned in a keyed location shown in Figure 6 (see callout D) such that the Newtonian secondary lens $\triangle 1$ * (Figure 5) directs the telescope primary lens focus toward the relay optics assembly $\triangle 2$. The actual primary focus (infinity focus) is 2 inches (5 cm) in front of the first lens (lens #1) of the relay optics assembly so that the received rays diverge to fill lens #1. Lens #1 collimates the diverging beam which then is focused by lens #2 onto the detector chip. The relay optics expand the field-of-view of the receiver to match the transmit beam divergence, and enables the use of a smaller detector with lower noise. The detector chip is 0.114 mm square and with the f/2 and f/1 relay lenses yields a receiver field-of-view of 1.23 mrad. To reduce sidelobe clutter such as that encountered in the Dugway 10.6 μm lidar system, the desirable field-of-view is equal to or slightly greater than the beam divergence of the laser.

* Numbers enclosed by triangles refer to components identified in Figure 5.

The relay optic assembly ② is mounted in a 5-axis precision optical mount ③ that allows precise alignment of this assembly. Alignment of the assembly is discussed in Appendix F. Once aligned, no further adjustments of this assembly should be required. In order to focus the receiving telescope at various ranges and provide a fine convergence adjustment for the transmit/receive system, the relay optic assembly/mount ② / ③ and detector/amplifier enclosure ④ are mounted on an X-Y-Z translation stage ⑤ .

The receiver electronics located in the RFI-tight enclosure provide detector bias and linear or logarithmic amplification of the received signal. If linear operation is selected, a maximum dynamic range of 40 dB (optical power) is available at the receiver package output. This linear dynamic range, however, cannot be appreciated when converting it to digital information because of digitizer limitations. Generally, only approximately 23 dB of this dynamic range can be utilized accurately in an 8-bit digitizer. Using the logarithmic amplifier over four decades, more than 40 dB of optical power can be digitized on an 8-bit digitizer system.

The specifications for the linear amplifier and log amplifier are given in Appendix G and H, respectively, and a schematic diagram of the receiver package electronics is given in Appendix I. Although logarithmic operation generally is desired, there are many applications where the greater accuracy required can only be achieved by linear amplification.

The video output (log or linear) from the receiver package is digitized by a Biomation 8100 that can be operated at a digitizing rate up to 100 MHz (10 ns sample rate). Specifications of the 8100 digitizer are found in the system equipment manual.¹¹ The digital output from the Biomation unit can be interfaced with the post-processing and/or recording equipment. Originally it was planned to interface this output with the data processing equipment of the LDV system located in a separate computer van but, during the course of the ASL lidar development, the LDV computer van became dedicated to other ASL programs. Thus, other approaches to recording and processing of the data must be examined.

IV SYSTEM IMPROVEMENTS

The overall objective in the ASL lidar developments was to improve system performance with respect to the prototype system used during the Dugway field test; specific attention was directed at improving range resolution, timing jitter, dynamic range, and reduction in sidelobe clutter. A comparison between the ASL lidar performance and the prototype system in the specific areas noted above follows:

(1) Range resolution--An improvement in range resolution from approximately 75 to 25 m was achieved by reducing the laser pulsewidth from 250 ns to 75 ns (FWHM). This improvement primarily was the result of careful characterization of the laser operation with a zero-N₂ gas mixture (Appendix E). The receiver system bandwidth also was increased from 10 MHz (receiver limitation) to 25 MHz (digitizer analog bandwidth) so that the shorter pulse width of the transmitted signal can be appreciated.

(2) Timing jitter--Unstable zero-time (laser has fired) triggering was the cause of the range jitter observed in the Dugway test data. This jitter primarily was caused by RFI coupled to the trigger line when the CO₂ laser discharge occurred. The use of a fiber optic pick-up of the laser spark gap discharge greatly reduces the problem in the ASL lidar system.

(3) Dynamic range--The prototype system used the SRI Mark IX lidar log amplifier on a time-share basis during the Dugway test. A log video amplifier improved in both risetime/falltime and dynamic range was developed for the ASL lidar system (Appendix H).

(4) Sidelobe clutter--Sidelobe clutter noted in the Dugway data was due to the fact that some transmitted energy (approximately 10%) is radiated outside the 1.2-mrad beam divergence specification. Some low-level energy may exist several mrad beyond the stated beam divergence. If scatter mechanisms are present along the path, some backscatter will occur even though they are outside the transmitter normal beam path. The amount of backscatter, of course, will depend on the type of scattering surface. At Dugway guy wires near the center of the optical path caused notable backscatter. This off-axis backscatter is a problem only if it is within the field-of-view of the receiver system which, at Dugway, was 3 mrad. To eliminate this problem in the ASL lidar system, the receiver system was designed so that the field-of-view (1.23 mrad) is just slightly larger than the transmitter beam divergence of 1.2 mrad. The only problem in matching the transmit and receive beams in this manner is the critical alignment it requires. Fortunately, when a target is used, as in smoke and dust measurements, a convenient daily performance evaluation and convergence backscatter signal is available for checking the system alignments (see Appendix F).

REFERENCES

1. Uthe, E. E., "Lidar Observations of Smoke and Dust Clouds at 0.7- μ m and 10.6- μ m Wavelengths," Technical Report No. 1, ARO Contract DAAG29-77-C-0001, SRI Project 5862 (1978).
2. "Remote Monostatic Wind Measuring System," Final Report Contract DAAH01-75-C-1057 for U.S. Army Missile Command, Lockheed Missiles & Space Company, Inc. (1976).
3. Technical Manual for Model 5201C Memory Voltmeter, Rev. 1, Micro Instrument Company, Escondido, CA (1969).
4. Operation and Maintenance Manual for Pulse Generators, Models 801 and 802, Dytech Corporation, Santa Clara, CA.
5. Instruction Manual for Series 100-2 TEA CO₂ Laser System, Serial No. 1434, Lumonics Research Limited, Kanata (Ottawa) Ontario, Canada (1978).
6. Lumonics Research Limited, private communication (1979).
7. Instruction Manual for Helium-Neon Lasers, Models 142-147, Spectra-Physics, Mountain View, CA (1976).
8. Instruction Manual for Pyroelectric Joulemeter, Model J3, Molelectron Corporation, Sunnyvale, CA (1978).
9. Operating Instructions for Models 36-0401 and 36-4001 Laser Power Meters, Scientech, Inc., Boulder, CO (1977).
10. Test Report No. 30270-1 for LK146 C9 S/N R-2 Infrared Detector for SRI International, Contr. No. A38923, Honeywell, Inc., Lexington, MA (1978).
11. Operating and Service Manual for Waveform Recorder, Model 8100, S/N 11930, Biomation, Santa Clara, CA (1978).

Appendix A
PERFORMANCE PREDICTION CALCULATIONS

Appendix A

PERFORMANCE PREDICTION CALCULATIONS

Calculations of signal-to-noise ratio (SNR) as a function of range have been made for the ASL lidar to establish expected system performance. The backscatter coefficient measured at Dugway Proving Grounds in 1977 was used for the calculation since atmospheric conditions are expected to be similar to those at White Sands, New Mexico where the first ASL lidar system evaluation was conducted.

To determine the SNR at a given range the lidar equation first is solved for backscatter signal:

$$P_r(R) = U_t \frac{A_r}{R^2} \frac{\lambda}{2h} \beta_{180} T_a^2 T_s \quad (1)$$

where

P_r = return signal, photon/s

U_t = transmitted energy, J/pulse

A_r = area of receiver, m^2

R = range, m

λ = wavelength, m

h = Planck's constant, 6.63×10^{-34} J-S

β_{180} = backscatter coefficient, $m^{-1} \text{sr}^{-1}$

T_a = atmospheric transmission = e^{-kr} , $k \sim 0.09 \text{ km}^{-1}$

T_s = system efficiency.

For this calculation, the following parameters were used:

$$U_t = 0.25 \text{ J/pulse}$$

$$A_r = 0.07297 \text{ m}^2 \text{ (12-in diameter)}$$

$$\lambda = 10.6 \text{ } \mu\text{m}$$

$$\beta_{180} = 7.4 \times 10^{-9} \text{ m}^{-1} \text{str}^{-1}$$

$$T_a = 0.91$$

$$T_s = 0.78.$$

The resultant received power levels were:

$$P_r (500 \text{ m}) = 5.576 \times 10^{-8} \text{ W}$$

$$P_r (1 \text{ km}) = 1.326 \times 10^{-8} \text{ W}$$

$$P_r (1.5 \text{ km}) = 5.61 \times 10^{-9} \text{ W}$$

$$P_r (2 \text{ km}) = 3.0 \times 10^{-9} \text{ W}.$$

The backscatter signal as a function of range then is compared with the receiver system noise equivalent power (NEP) which is derived from the detector and receiver characteristics as follows:

$$\text{Detector NEP} = \frac{\sqrt{A}}{D^*} = 2.6 \times 10^{-12} \text{ W}/\sqrt{\text{Hz}}$$

where A = detector area $1.14 \times 10^{-3} \text{ cm}^2$ and $D^* = 1.3 \times 10^{10} \text{ cmHz}^{1/2} \text{ W}^{-1}$.

With a receiver bandwidth of 25 MHz the system NEP = $1.3 \times 10^{-8} \text{ W}$.

Comparing the system NEP with the anticipated received power, we can see that an SNR = 1 is expected at a range of 1 km.

Appendix B

SCHEMATIC FOR CONTROL UNIT

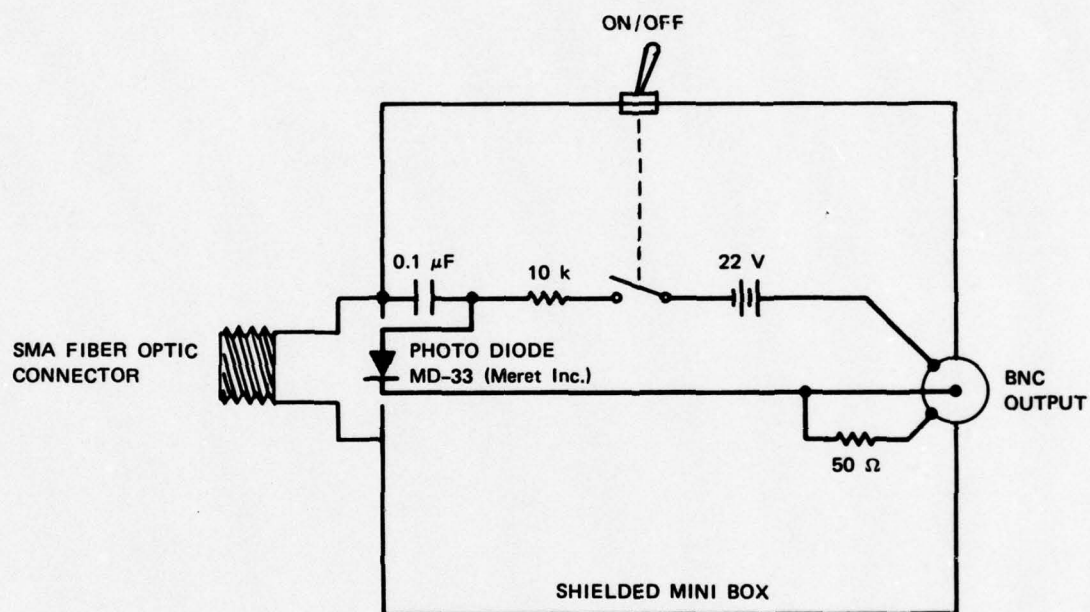


Appendix C

SCHEMATIC FOR TRIGGER AND SYNCHRONIZED
PULSE ISOLATION INTERFACE

Appendix D

SCHEMATIC FOR FIBER OPTIC DETECTOR UNIT



APPENDIX D SCHEMATIC FOR FIBER OPTIC DETECTOR UNIT

Appendix E
LASER OPERATING CONDITIONS

Appendix E

LASER OPERATING CONDITIONS

Operation of the Lumonics CO₂ laser system for minimum pulsewidth output requires operation with fundamental transverse mode optics (unstable resonator cavity) and zero-nitrogen (N₂) lasing gas mix. For stable operation under these conditions there is a definite optimum gas mixture, gas flow rate, and high voltage setting for each selected PRF rate. The ASL lidar laser was optimized for operation at a 1-Hz PRF rate, and the following conditions produced a 250-mJ, 75-ns (FWHM) pulse output with a pulse-to-pulse amplitude stability better than $\pm 5\%$:

He regulator pressure	10 lb
CO ₂ regulator pressure	10 lb
He flow rate	7 (flowmeter reading)
CO ₂ flow rate	3 (flowmeter reading)
High voltage	38 kV

The Lumonics Operation Manual should be consulted for general operating hints and instructions.

Appendix F

RECEIVER ALIGNMENT PROCEDURE

Appendix F

RECEIVER ALIGNMENT PROCEDURE

The alignment procedure described here is a complete receiver system alignment and generally will be required only during initial setup of the lidar system. During normal operation a routine standard lidar convergence adjustment is all that is required. If a lidar target is to be used during normal operation, the target return will provide an excellent system performance reference as well as a convenient convergence signal. A convergence procedure also is discussed in this receiver system alignment outline.

The ASL lidar receiver system is aligned when the receiver detector or its image is on the principal axis and at the focal point of the receiver telescope primary. The principal axis of the telescope also must be centered on the transmit/receive (T/R) steering mirror. To achieve this alignment, the first step is to confirm that the telescope primary and the T/R steering mirror are in proper alignment (this condition should exist if the LDV system is aligned).

Step A.

1. Place a retroreflector cube on a stand at a range of 100 m from the van on or near the anticipated optical path of interest.
2. Illuminate the retroreflector with the HeNe transmit alignment laser by steering the beam with the T/R steering mirror on to the retroreflector (it is assumed that the transmit system is aligned, and

that the HeNe alignment laser defines the IR optical path). If the telescope primary is aligned properly an image of the illuminated retroreflector will be seen on a white card held 9 inches above and 9 inches from the edge of the optical table and approximately two ft in front of the primary.

3. If the retroreflector image is not seen at the desired location the primary mirror should be adjusted so that it is. To aid in this adjustment, position the LDV secondary lens at the exact desired primary focus location.* Loosen the primary mirror lock-down screws and adjust the appropriate controls to position the retroreflector image at the center of the LDV secondary. Tighten the lock-down screws and confirm that the image has not moved; repeat procedure if necessary.

This completes the telescope primary adjustment.

Step B.

1. Place the lidar receiver package in its keyed location on the table and bolt it down.** In this location the lidar Newtonian secondary mirror, located on the receiver package, should direct the principal axis of the receiver 90° from the normal and towards the relay-optic housing on the receiver package. The retroreflector image should be located using a white card held approximately 2 inches in front of the relay optic housing.

* The LDV secondary is mounted on a special X-Y-Z translation mount and normally should be on the proper receiver axis; in order to focus the system at 100 m, only a Z-translation should be required.

** Prior to installing the receiver package, the optics of the relay optics assembly should be aligned and focused on the desired detector chip using the visible optic assembly provided. This assembly will be changed to a matching IR optics assembly in Step C.

2. If the retroreflector image (Step B-1) is not near the location expected, check its location with respect to the table and primary mirror. The image should be 19 inches in front of the primary mirror, 9 inches above and 4 inches from the edge of the table; if it is not, adjust the position of the Newtonian secondary.

3. The position of the entire detector/relay optic package now can be adjusted using the package X-Y-Z position controls so that the relay optics are on-axis and 2 inches beyond the focused retroreflector image. The package is placed 2 inches beyond the image focus because the relay optics provide a four-fold detector field-of-view expansion and the expanded detector image is located 2 inches in front of the relay optic assembly.

The basic visible receiver adjustments are now completed. The following adjustments are required to correct for any differences between the visible relay optic assembly and the IR optics assembly used in system operation.

Step C.

1. Replace the visible relay optic assembly with the IR optic assembly on the relay optic mount, being careful not to disturb any of the 5-axis adjustments.

2. Replace the retroreflector cube used in Steps A and B with a chopped IR source (a hair dryer element with a chopper blade and motor in front of the element makes an excellent IR source for this alignment).

3. Fill the LN_2 Dewar flask in the receiver package with LN_2 and turn the receiver on.

4. Connect an ac-microvolt meter (i.e., H-P 400E) to the receiver output. Do not use the log amplifier for this test. If the receiver is aligned properly, a detectable signal-to-noise change in receiver output level will be observed when the receiver beam is blocked and unblocked. The receiver "no signal" noise level output should be between 60 and 80 μ V. If no change is observed, translate the receiver package in the X-Y-Z axis until a signal is detected. Once a detectable level is observed and peaked, readjust the relay optic adjustments to optimize the signal. Only minor adjustments should be required.

The receiving system adjustments for system focus at 100 m are now completed. To focus the system at other ranges, calculate the required image position change from the 100 m location, and reposition the receiver package using the Z-axis adjustment. This should be a very minor adjustment since the 100 m-to-infinity change is only 3.8 mm. A more accurate focus adjustment, also serving as a complete receiver/transmitter alignment, is described in Step D.

Step D.

1. Align the receiver onto a target of interest using the T/R steering mirror. A focused image of the target should be seen near the telescope primary focus if a white card is placed at that location. Adjust the T/R steering mirror so that the target image is centered on the principal axis of the receiver. The receiver system now is aligned in X-Y coordinates on the target of interest.

2. Turn the CO₂ laser system on and illuminate the target.

The CO₂ laser output should be aligned on the target at this time since the transmit alignment HeNe laser (which defines the CO₂ laser path) was used to define the principal receiver axis in Step A of this procedure.

3. Connect the output of the receiver to a peak reading voltmeter (PRVM) and dual trace oscilloscope, and observe the return signal on the scope.

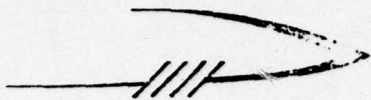
4. Put the PRVM gate signal on the second channel of the oscilloscope and adjust the gate range to the target location. A reading on the PRVM now should be seen and represents the peak amplitude return.

5. Be sure that the transmitter and receiver beams are in convergence by adjusting the last transmit steering mirror in X and Y. Each adjustment should be scanned while observing the PRVM for the maximum signal. Note the 50% amplitude location on each side of the peak signal for both the X and Y micrometer settings and set both micrometers for the mid-range position. Note that this lidar convergence adjustment generally is the only daily adjustment required.

6. Adjust the receiver package Z-position control for a maximum signal on the PRVM. The receiver system now is focused at the target range.

The receiver system alignment procedure is now completed.

Appendix G
SPECIFICATIONS FOR RECEIVER LINEAR AMPLIFIER



PERRY AMPLIFIER

WIDEBAND RF TRANSISTOR AMPLIFIER

ULTRA LOW NOISE FOR

LASER-PULSED DETECTOR SYSTEMS

MODELS 460 THRU 490

SPECIFICATIONS

GAIN ($R_G=50$ OHM) 26DB

BANDWIDTH ($R_G=50$ OHM)

MODEL 460	200HZ - 10MHZ
MODEL 470	200HZ - 30MHZ
MODEL 480	200HZ - 50MHZ
MODEL 490	200HZ - 100MHZ

PULSE RESPONSE 5 NANOSECONDS

INPUT IMPEDANCE 50 OHM

OUTPUT IMPEDANCE 2 OHM

OUTPUT LEVEL MAXIMUM 3 VOLTS P-P

POWER REQUIREMENTS $\pm 12V$ @ 20MA

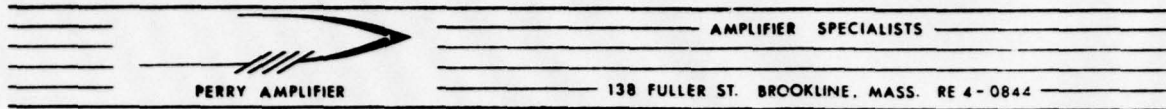
OPERATING TEMPERATURE $-55^{\circ}C$ TO $85^{\circ}C$

MECHANICAL SIZE 2" X 2" X 1"

THE SERIES 460 THRU 490 VIDEO PREAMPLIFIERS ARE SPECIALLY DESIGNED FOR USE WITH HIGH-SPEED PHOTODETECTORS IN PULSE AND CW LASER SYSTEMS. THESE UNITS WILL ACCEPT VARIOUS INPUT IMPEDANCES AS PRESENTED BY TYPICAL DETECTORS AND MAINTAIN OVERALL STABILITY AND PERFORMANCE WITH INPUTS FROM 10 OHM TO 1K OHM.

PERRY AMPLIFIER BROOKLINE, MASS. 617 - RE 4 - 0844

OPERATING INSTRUCTIONS
PLEASE READ CAREFULLY BEFORE OPERATING



MODEL 490 WIDEBAND VIDEO AMPLIFIER

INPUT- THE INPUT OF THE AMPLIFIER IS CAPACITIVELY COUPLED INTERNALLY WITH A 1UF CAPACITOR RATED AT 25 VOLTS NON-POLAR. TO EXCEED THIS VOLTAGE RATING ADD AN EXTERNAL CERAMIC TYPE CAPACITOR.

THE INPUT IMPEDANCE IS 50 OHMS. THE AMPLIFIER IS STABILIZED TO ACCEPT INPUT DRIVING IMPEDANCES OF 10 OHM TO 1K OHM. OPTIMUM AMPLIFIER PERFORMANCE IS ATTAINED WITH RESISTIVE DRIVE SOURCES. MOST DETECTORS ARE HOWEVER REACTIVE IN NATURE DUE TO INTRINSIC DETECTOR CAPACITANCE. IT IS RECOMMENDED THAT THE INPUT DRIVING CAPACITANCE BE KEPT AT A MINIMUM TO MINIMIZE REFLECTIVE DISTORTION AND INSTABILITY. SHORT CABLES ARE A MUST. HIGHLY REACTIVE DETECTORS REQUIRE SPECIAL COMPENSATION FOR OPTIMUM PERFORMANCE, THEREFORE IT IS OFTEN ADVISABLE TO DETERMINE THE EXACT ELECTRICAL CHARACTERISTICS OF THE DETECTOR AND HAVE THEM MATCHED SPECIFICALLY TO THE AMPLIFIER.

OUTPUT THE OUTPUT OF THE AMPLIFIER IS CAPACITIVELY COUPLED INTERNALLY WITH A 3UF CAPACITOR. SHORT CIRCUITS WILL NOT DAMAGE THE AMPLIFIER WHEN OPERATING AT LOW SIGNAL LEVELS. THE OUTPUT IMPEDANCE @100MHZ IS 50 OHMS. THE BASIC MODEL 490 WILL DRIVE 50 OHM CABLES OF SHORT LENGTH TO A MAXIMUM OF 1 VOLT PEAK INTO 50 OHMS. TO DRIVE LONGER CABLES IT IS RECOMMENDED THAT A PERRY VIDEO LINE DRIVE BE INSTALLED. INSTALLATION OF THE LINE DRIVE EXPANDS THE OUTPUT CAPABILITY TO 4 VOLTS PEAK, EXTENDS LOW

FREQUENCY RESPONSE AND RETRIEVES 6DB GAIN LOST IN THE LOADING EFFECT OF THE 50 OHM TERMINATION. A VIDEO LINE DRIVER CIRCUIT CAN BE INSTALLED IN SOME VERSIONS OF THE MODEL 490. SUCH UNITS ARE SPECIAL DESIGNS FOR SPECIFIC AMPLIFICATIONS AND DESIGNATED AS MODELS 490LD.

GAIN THE VOLTAGE GAIN OF THE AMPLIFIER IS A FUNCTION OF THE INPUT DRIVING SOURCE IMPEDANCE. THE GAIN IS 26DB @ 50 OHM DRIVING SOURCE IMPEDANCE, AND WILL DECREASE SOMEWHAT WITH HIGHER SOURCE IMPEDANCES.

TANDEM OPERATION IN MANY CASES ADDITIONAL GAIN MAY BE REQUIRED TO MEET SYSTEM DEMANDS. IT IS POSSIBLE TO DIRECTLY STACK TWO MODEL 490 BY DIRECT CONNECTION TO GIVE OVERALL GAIN OF 50DB. TANDEM OPERATION WILL CAUSE SOME CONTRACTION OF BANDWIDTH AS IS TO BE EXPECTED.

POWER REQUIREMENTS THE POWER SUPPLY SHOULD BE OF GOOD DESIGN TO ELIMINATE POWER SUPPLY FEEDBACK. TWIST ALL POWER LEADS TO THE AMPLIFIER AND BY-PASS THE POWER AT THE AMPLIFIER WHENEVER POSSIBLE. CURRENT DEMAND WILL VARY FROM UNIT TO UNIT WITH A 16MA AVERAGE. MODEL UNITS 490LD WILL REQUIRE 40MA CURRENT @ ± 12 VOLTS. BIAS CIRCUITS SHOULD BE INDEPENDENT OF AMPLIFIER POWER CIRCUITS. USE SEPARATE BATTERIES FOR IDEAL ISOLATION AND NOISE MINIMIZATION.

CAUTION : DO NOT CONNECT POWER TO THE AMPLIFIER IN REVERSE. REVERSE POWER WILL DAMAGE THE AMPLIFIER.



ENGINEERING NOTE: MODEL 490 SERIAL NO. 6861 RF AMPLIFIER.

THIS UNIT HAS BEEN OPTIMIZED FOR USE WITH A HONEYWELL DETECTOR IMPEDANCE RANGE 50 TO 200 OHMS/ 10PF CAPACITANCE. THE MODULE CONTAINS A FIXED DECOUPLED BIAS RESISTOR TO SUPPLY BACK BIAS TO THE DETECTOR DIODE. THE BIAS RESISTOR VALUE IS 24K OHM AND WILL SUPPLY 500UAMP TO THE DETECTOR WHEN OPERATED FROM A 12 VOLT BATTERY SOURCE. THE BIAS CIRCUIT IS ACCESSABLE VIA TERMINAL MARKED "V". APPLY BIAS ONLY WHEN DETECTOR IS SECURELY CONNECTED TO AVOID INPUT VOLTAGE OVERLOAD.

G. PERRY

24

Appendix H
SPECIFICATIONS FOR RECEIVER LOGARITHMIC AMPLIFIER

PLAMIC

PLANAR MICROWAVE INTERNATIONAL CORPORATION

A DIVISION OF THE KURAS-ALTERMAN CORPORATION

138 KIFER COURT, SUNNYVALE, CALIFORNIA 94086 (408) 739-3400

Log Video Amplifier

P/N LVA 1010 EP

S/N 801

Specification

Measured

1. Input Impedance 50Ω

50 Ω

2. Output Slope
21 mv/db (nom)

20.5 mv/db

3. Risetime 15 n sec.

Those
figures
include
test
equipment
risetimes

22 ns (-81 dbr)

16 ns (-51 dbr)

15 ns (-31 dbr)

15 ns (-11 dbr)

4. Settling time 30 n sec.

32 ns (-81 dbr)

28 ns (-51 dbr)

28 ns (-31 dbr)

~ 30 ns (-11 dbr)

Cog. Engineer Ron Canaris

Date 8/4/78

Q.A. J. Shom

Date 8/4/78

Product Line Manager _____

Date _____

Tested By Ron Canaris

Date 8/4/78

Q.A. J. Shom

CABLE ADDRESS: PLAMIC • TWX: 910-339-9220

Appendix H 1 of 3

PLAMIC

PLANAR MICROWAVE INTERNATIONAL CORPORATION

A DIVISION OF THE KURAS-ALTERMAN CORPORATION
138 KIFER COURT, SUNNYVALE, CALIFORNIA 94086 (408) 739-3400

S/N 801

Specification

5. Output s/n ratio at 200 mv
input, less than 16 db.

6. Log conformity ± 0.5 db

7. Recovery Time:

Direct and indirect measurements have been made which verify that the unit will recognize a low level pulse following a high level pulse within 50 nanoseconds. Recovery time however, is difficult to measure because the test and measurement equipment cannot generate or measure the extremely high on-to-off ratios required to properly evaluate the device being tested. This problem was discussed with Jon Vanderlawn.

Measured

*Tangential Signal
Sensitivity 211 db*

see attached transfer
response

Tested By:

Ram Canario

Date:

8/4/78

Q.A.:

J. Thomas

CABLE ADDRESS: PLAMIC • TWX: 910-339-9220

Appendix H 2 of 3

PLAMIC

PLANAR MICROWAVE INTERNATIONAL CORPORATION

A DIVISION OF THE KURAS-ALTERMAN CORPORATION

138 KIFER COURT, SUNNYVALE, CALIFORNIA 94086 (408) 739-3400

S/N 801

Transfer Response

10 volt input signal defined as 0 dbr

Input (dbr)	Output (mv)	Error (db)
-1	1997	-.42
-6.15	1902	+.1
-11.15	1788	-.45
-16.3	1691	-.02
-21	1598	+.147
-26.15	1494	+.08
-31	1395	+.26
-36.15	1290	+.29
-41	1179	-.26
-46.15	1086	+.356
-51	986	+.335
-56.15	874	+.03
-61	776	+.1
-65.15	683	-.27
-71	567	-.07
-76.15	460	-.14
-81.1	362	+.04
-86.25	252	-.17
-91.15	153	-.1

Tested By: Ron Cincio Date: 8/4/78

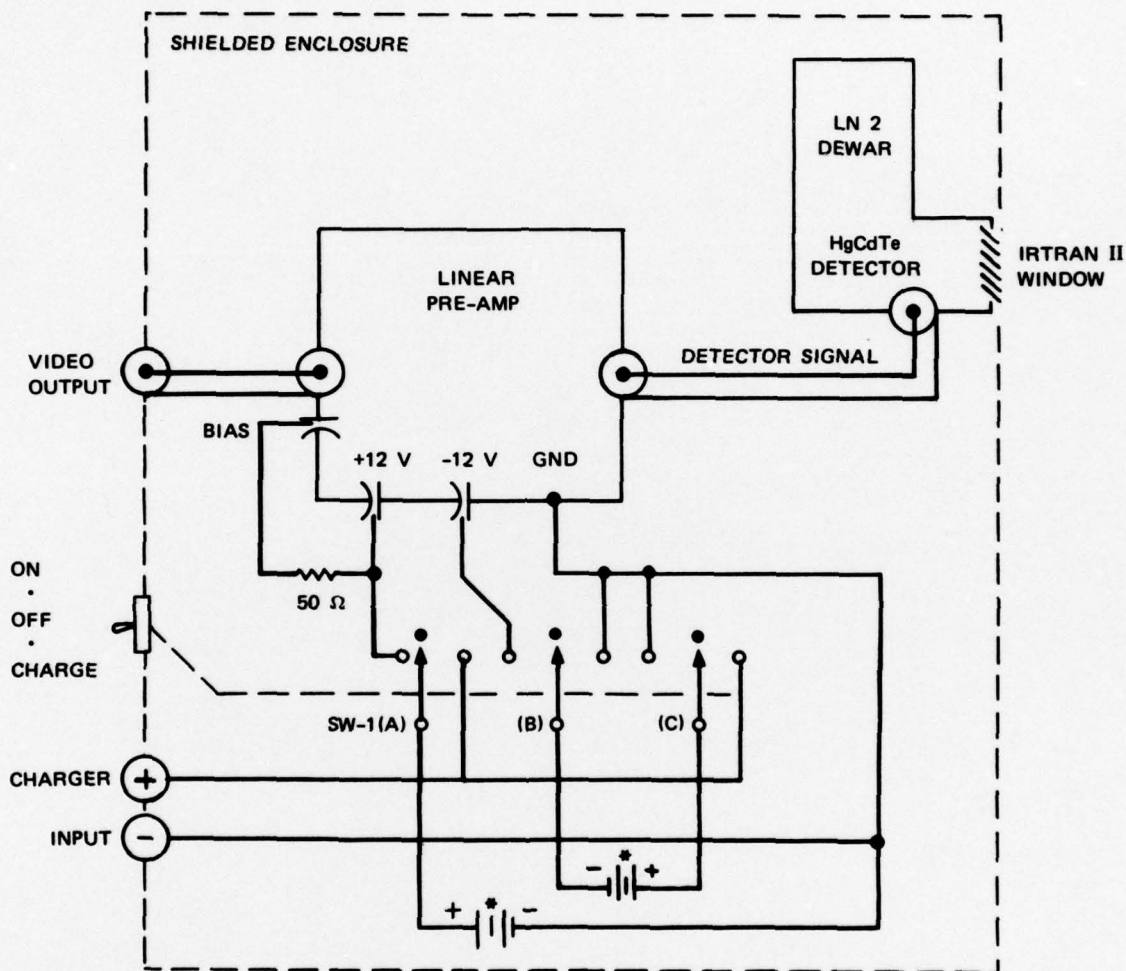
Q.A. J. Johnson

CABLE ADDRESS: PLAMIC • TWX: 910-339-9220

Appendix H 3 of 3

Appendix I

RECEIVER ELECTRONICS PACKAGE WIRING DIAGRAM



* 12 V/2.5 Ah
RECHARGEABLE BATTERY PACK
(Gates 810.0016)

APPENDIX I RECEIVER ELECTRONICS PACKAGE WIRING DIAGRAM